Nucleic Acids Research, 2006, Vol. 34, No. 13 ***3731–3741***
doi:10.1093/nar/gkl554

Role of ATP hydrolysis in the DNA translocase activity of the bovine papillomavirus (BPV-1) E1 helicase

Sandrine Castella, David Burgin and Cyril M. Sanders*

Institute for Cancer studies, University of Sheffield, Beech Hill Road, Sheffield S10 2RX, UK

Received May 30, 2006; Revised July 10, 2006; Accepted July 17, 2006

ABSTRACT

The E1 protein of bovine papillomavirus type-1 is the viral replication initiator protein and replicative helicase. Here we show that the C-terminal ~300 amino acids of E1, that share homology with members of helicase superfamily 3 (SF3), can act as an autonomous helicase. E1 is monomeric in the absence of ATP but assembles into hexamers in the presence of ATP, single-stranded DNA (ssDNA) or both. A 16 base sequence is the minimum for efficient hexamerization, although the complex protects ~30 bases from nuclease digestion, supporting the notion that the DNA is bound within the protein complex. In the absence of ATP, or in the presence of ADP or the non–hydrolysable ATP analogue AMP–PNP, the interaction with short ssDNA oligonucleotides is exceptionally tight ($T_{1/2}$ > 6 h). However, in the presence of ATP, the interaction with DNA is destabilized ($T_{1/2}$ ~60 s). These results suggest that during the ATP hydrolysis cycle an internal DNA-binding site oscillates from a high to a low-affinity state, while protein–protein interactions switch from low to high affinity. This reciprocal change in protein–protein and protein–DNA affinities could be part of a mechanism for tethering the protein to its substrate while unidirectional movement along DNA proceeds.

INTRODUCTION

Helicases couple the energy of nucleotide hydrolysis to the unwinding of double-stranded nucleic acids. Many of these enzymes function as oligomers including the viral helicases T-antigen and E1, the replicative helicases of SV40 (1,2) and papillomavirus, respectively (3,4). These proteins are also the initiator proteins that first melt the origin DNA (*ori*) where they then assemble as helicases (5,6). The melting of duplex DNA and processive unwinding are distinct processes, but there are indications of mechanistic similarities. This is based largely on a shared requirement for amino acids in the helicase domains (HDs) of SV40 and E1 that form a single-stranded DNA (ssDNA) binding site (7,8). DNA melting occurs at specific sites defined by the origin-recognition sequence (*ori*) and the sequence-specific-origin binding domains (OBDs) of these initiators. In bovine papillomavirus (BPV-1) the E1 protein assembles in a stepwise fashion on *ori* (9). The initial binding of E1 as a dimer requires the assistance of the transcription factor E2 (10), which orientates subsequent oligomeric complexes in a head to tail array. In the presence of ATP, oligomers from tetramer through to double hexamers have been observed (11,12). In the absence of ATP, the E1–*ori* complexes that form are relatively unstable. Two E1 trimers melt the DNA either side of the E1-binding site. This event is ATP dependent and requires the cooperation of the OBD and an ssDNA-binding site in the E1HD. The final transition to the putative double hexameric replicative helicase is not understood. However, the predicted rearrangement to two protein rings is likely to require the ongoing involvement of the ATP-modulated ssDNA-binding site in the E1 helicase domain (E1HD). In SV40, T-antigen also assembles on *ori* in various oligomeric states (13), but the *ori* melting complex structure has not been defined.

The hexameric helicases studied to date bind both ssDNA and dsDNA as ring-shaped structures. In most cases ssDNA is the preferred substrate for DNA binding. As described above, the high affinity of T-antigen and E1 for dsDNA is primarily a manifestation of the presence of the OBD, and related to the assembly process for concentrating the proteins at *ori*. For T7 gp4, *Escherichia coli* DnaB helicase and other members of the DnaB family, ssDNA binds in a central cavity generated by oligomerization (14–17). Binding appears unidirectional, consistent with the defined unwinding polarity of helicases (14). Binding to replication forks, which is likely to reveal important features of the helicase mechanism, has been studied less extensively. However, DNA footprinting studies suggest that T-antigen encircle one DNA strand at a replication fork structure with interactions extending into the duplex region ahead of the fork. The other DNA strand is excluded from the protein complex (18,19). Quantitative fluorescence titration studies with synthetic replication forks demonstrate that DnaB also excludes one strand of DNA when the substrate is engaged (20). The requirements for oligomerization of hexameric helicases differ, although in most cases a

*To whom correspondence should be addressed. Tel: +44 114 2712482; Fax: +44 114 2713892; Email: c.m.sanders@sheffield.ac.uk

nucleotide is required. T-antigen forms hexamers with ADP, ATP and non-hydrolysable analogues (21). For bovine papillomavirus (BPV) E1 it has been reported that the enzyme purified from *E.coli* requires DNA for hexamerization, with or without ATP (22), but the enzyme purified from recombinant baculovirus-infected insect cells exists in a number of oligomeric states (23). Similar results have been reported for HPV 11 E1 from insect cells infected with a recombinant baculovirus (24).

The helicase mechanism can be viewed as a DNA translocase activity coupled to a base pair separation process. However, how these processes proceed mechanistically and are coupled to each other and NTPase activity are largely unknown. Mechanisms based on active and passive unwinding have been proposed but differentiating between them is problematic since they share common features, principally the modulation of protein–protein and protein–DNA interactions in a nucleotide hydrolysis cycle (25). Here we report the characterization of the enzymatic, oligomerization and DNA-binding properties of a helicase protein derived from the C-terminal domain of BPV E1. The E1HD is monomeric but assembles into hexamers with ssDNA or ATP but not ADP or AMP–PNP. The minimal DNA-binding site size for efficient oligomerization is ~16 bases. With ADP, AMP–PNP or without a cofactor hexamers form an exceptionally tight complex with ssDNA. However, in the presence of ATP the half-life of the protein–ssDNA interaction is, comparatively, exceptionally short. These results suggest that during the ATP hydrolysis cycle an ssDNA-binding site ocillates from a high to a low-affinity state whereas protein–protein interactions change from a low- to high-affinity state. These features are indicative of an ssDNA translocase activity, thus defining a component of the helicase mechanism for this important viral protein.

MATERIALS AND METHODS

Protein expression, purification and quantification

DNA encoding the C-terminal 308 codons of BPV E1 was cloned into the NdeI/BamHI sites of pET11c for expression in *E.coli* BL21(DE3), induced with 0.4 mM isopropyl-β-D-thiogalactopyranoside (IPTG) at 20°C for 6 h. Cells were lysed by lysozyme treatment (0.5 mg/ml, 30 min at 4°C) followed by sonication in 50 mM Tris–HCl, pH 8.0 (4°C), 0.4 M NaCl, 10 mM EDTA, 10 mM DTT, 10% (v/v) glycerol and 1 mM phenylmethanesolphonyl fluoride (PMSF), at 3 ml/g of cells. The extract was cleared at 40 000× *g*, and the E1HD was precipitated with polyethylenamine P (0.5%, w/v) and re-solubilized with lysis buffer containing 1.5 M NaCl. The extract was adjusted to 20% saturation (4°C) with ammonium sulphate and applied to a butyl-sepharose column equilibrated with 40 mM sodium phosphate, pH 6.2, 1 mM EDTA, 10% (v/v) glycerol, 2.5 mM DTT, 0.1 mM PMSF and 0.7 M $(NH_4)_2SO_4$. Protein was eluted in a gradient to 0.1 M $(NH_4)_2SO_4$. Peak fractions were dialysed against buffer S [20 mM sodium phosphate, pH 6.8, 2.5 mM DTT, 0.5 mM EDTA, 10% (v/v) glycerol and 0.1 mM PMSF] containing 100 mM NaCl. Protein was further purified on a Source-S column (Amersham-Pharmacia), on a gradient from 50 to 350 mM NaCl. Peak fractions were pooled and applied to a Sephacryl S100 size exclusion column equilibrated in 20 mM sodium phosphate, pH 7.0, 200 mM NaCl, 0.1 mM EDTA, 10% (v/v) glycerol, 2 mM DTT and 0.1 mM PMSF. Peak fractions were further purified on a Source Q column as described for full-length E1 (26). Peak fractions were pooled, dialysed against 100 mM HEPES, pH 7.5, 200 mM NaCl, 5 mM DTT and 5% (v/v) glycerol, concentrated and stored at −80°C. Full-length BPV E1 was purified as described previously (26).

E1HD protein concentration was determined by A_{280} nm in 6 M guanidinium hydrochloride using the molar extinction coefficient (ε) of 56 030 cm^{-1} M^{-1}. A standard curve using the Bio-Rad reagent (Bio-Rad) was constructed using absolute values of protein concentration determined in this way. E1 concentrations were determined by Bio-Rad assay.

ATPase assays

ATPase assays were performed in 20 mM HEPES–NaOH, 135 mM NaCl, 1 mM DTT, 0.01% (v/v) NP-40, 7.5 mM ATP and 8.5 mM $MgCl_2$ containing 35 nmol/μl [γ-^{32}P]ATP (7000 Ci/mmol) and the protein concentrations given. Reactions were incubated at 22°C and P_i release determined by the charcoal-binding assay described by Iggo and Lane (27).

Helicase assays

Helicase reactions were performed in 25 mM HEPES–NaOH, 20 mM NaCl, 1 mM DTT, 1 mM ATP and 3 mM $MgCl_2$ as described previously (8). For the polarity assay, the substrates each comprises 64 bases of dsDNA with either a 5′ or 3′ 48 base overhang. Reactions were incubated at 22°C for 60 min and terminated by adjusting the reactions to 20 mM EDTA, 0.1% (w/v) SDS, 10% (v/v) glycerol and 0.13% (w/v) bromophenol blue. Products were separated on 8% polyacrylamide/TBE gels containing 0.05% (w/v) SDS, and gels exposed to phosphorimager plates (Fujifilm) for imaging and quantification (Fuji FLA3000; image gauge V3.3 software).

To determine the ability of E1HD to displace long DNA fragments from duplex DNA, a ^{32}P-end-labelled primer, 5′-CTTGCATGCCTGCAGGTCGACTCT was annealed to single-stranded M13 DNA and extended using SequiTherm *Taq* polymerase (Epicentre) with a nucleotide mixture containing 25 μM each dATP, dCTP, dTTP, 7-deaza-dGTP and 170 μM ddCTP. The substrate was passed through a G25 desalting column (Amersham-Pharmacia). The substrate concentration in helicase reactions was 1 nM with the stated concentrations of helicase protein. Human RPA was expressed and purified as described in (28). Reactions (40 μl) were incubated at 22°C and terminated by the addition of 200 μl of 0.5 M ammonium acetate, 1 mM EDTA, 0.1% (w/v) SDS, phenol–chloroform extracted, ethanol precipitated, dried and dissolved in 20 μl of 1× TBE electrophoresis buffer/2 M urea. Products were analysed on a 5% 7 M urea–polyacrylamide sequencing gel (TBE running buffer) without heating. The temperature of the gel was maintained at 30–35°C during the run. Under these conditions, sequence ~>40 bases do not spontaneously dissociate. The dried gel was imaged as described above.

DNA-binding reactions

Poly(dT) oligonucleotides were purchased from Sigma and end-labelled with polynucleotide kinase and [γ-^{32}P]ATP (7000 Ci/mmol). The binding buffer was 20 mM sodium phosphate, pH 7.2, 135 mM NaCl, 10% (v/v) glycerol, 0.1% (v/v) NP-40, 0.1 mg/ml BSA, 1 mM PMSF, 1 mM DTT and the probe concentration 1–2 nM unless otherwise stated. Reactions were performed at 22°C. In some reactions ATP/Mg^{2+}, ADP/Mg^{2+} and AMP–PNP/Mg^{2+} were at 5 mM. Reaction products were resolved on 5% 80:1 acrylamide/bisacrylamide gels using 0.25× TBE as the electrophoresis buffer. In some instances (half-life determinations, Figure 6), protein–DNA complexes were first cross-linked with 0.8×10^{-3}% (v/v) glutaraldehyde for 5 min followed by quenching with Tris–HCl to 80 mM. Imaging and quantification were as described above. A double-stranded 30 base T–A duplex was generated by annealing a labelled poly(T) strand to the adenine polynucleotide. All labelled probes were purified from native polyacrylamide gels. Gels were exposed to phosphorimager plates for visualization and quantification. Dissociation constants (K_d) were determined after saturation was reached by fitting a four-parameter logistic equation (Hill's equation) to the data using GraphPad Prism 4 software. In all cases R^2 was $\geqslant$0.99.

DNA protection assay

An 84 bp PCR product was generated form the wild-type BPV *ori* template described in (29) with the following primers: 5′-GTAAAACGACGGCCAGT and 5′-GGAAAAAATACATAGTCTTTAC, the latter primer being phosphorylated with polynucleotide kinase. The PCR (100 µl) contained 200 µM dATP, dGTP and dCTP, 20 µM dTTP and ~50 pmol [α-^{32}P]dTTP (3000 Ci/mmol). The final PCR product was treated with λ exonuclease to degrade the 5′ phosphorylated strand, and the ssDNA product phenol–chloroform extracted and ethanol precipitated. Binding reactions with the E1HD (50 µl) were performed as described above and treated with ~30 U each of nuclease P1 and micrococcal nuclease (22°C). Reactions were terminated by the addition of an equal volume of formamide (98%, v/v) loading buffer and analysed directly on 12% urea–polyacrylamide sequencing gels. A marker ladder was created with end-labelled synthetic oligonucleotides.

Gel filtration and glycerol gradient centrifugation

Gel filtration was performed using a Superdex S-200 column (Amersham Bioscience) equilibrated in 20 mM sodium phosphate, pH 7.2, 200 mM NaCl, 10% (v/v) glycerol, 1 mM PMSF, 1 mM DTT and either no cofactor, ATP 1 mM/3 mM $MgCl_2$ or 1 mM ADP/3 mM $MgCl_2$. The column was calibrated using the size markers, ferritin (440 kDa), catalase (232 kDa), aldolase (158 kDa), BSA (67 kDa) and carbonic anhydrase (29 kDa). In some instances, proteins were pre-incubated in the presence of 5 mM ATP/Mg^{2+} or 5 mM ADP/Mg^{2+} (100 µl reactions, 4°C) for 10 min before sample injection and development of the column at a flow rate of 0.5 ml/min. Protein elution was monitored at 280 nm and chromatograms analysed using computer software (Unicorn V4.0; Amersham Bioscience). Glycerol gradient sedimentation was performed on 20–40% (v/v) gradients in the same buffer used for gel filtration, but also one containing AMP–PNP 1 mM/3 mM $MgCl_2$, and gradients were calibrated with the same markers run in parallel. Gradients were spun for 16 h at 50 000× *g*, 4°C in a Beckmann SW55 rotor. Fractions were run on 12% SDS–PAGE gels, and sedimentation profiles analysed by densitometry (digitized images, Kodak ID 3.5.4 software). Molecular weight calculations (method of Siegel and Monty) were performed as described previously (30).

To determine the molar ratio of protein to DNA in the E1HD–DNA complex, protein–DNA complex formation was initiated using a ^{32}P-radiolabelled oligonucleotide, and reactions fractionated by gel filtration. The protein concentration of the peak fraction was measured by Bio-Rad assay. An exact value for protein concentration was determined from a standard curve generated with protein amounts measured by A_{280} under denaturing conditions (6 M guanidinium hydrochloride; ε 56 030 cm^{-1} M^{-1}). The DNA content of the peak fraction was determined by comparing radioactive emission against a standard dilution series of the labelled oligonucleotide used for protein–DNA complex formation.

RESULTS

Helicase activity of E1HD

We purified to near homogeneity a recombinant E1HD protein, E1HD, comprising the C-terminal 307 amino acids of E1 (Figure 1a and b). The start point of this construct was defined by the end point of the sequence-specific E1 OBD, and is ~30 amino acids upstream of the sequence alignment with SV40 and polyoma virus T-antigens. We first asked if E1HD retained the polarity of DNA unwinding of full-length E1 (Figure 1c). Helicase substrates with 64 bp of double-stranded DNA and either a 3′ or 5′ 48 base overhang were generated, with the 64 base fragment ^{32}P-end-labelled. Lanes 1 and 2 show the native and denatured substrate. Recombinant E1HD (lanes 3–7) and E1 (lanes 8–10) both displaced the labelled oligonucleotide from the substrate with the 3′ overhang, but not the 5′ overhang (Figure 1c, left and right, respectively). DNA substrates of pure duplex character were not unwound by the enzyme (data not shown). We note also that high-protein concentrations appeared inhibitory for unwinding. Next, we asked if E1HD was capable of unwinding long DNA substrates. An end-labelled primer was annealed to single-stranded M13 DNA and extended with all four dNTP and a pre-defined ratio of ddCTP to dCTP, generating a series of extension products. Figure 1d, lanes 1 and 2 are size markers. Lane 3 is the labelled primer, and lane 4 the extension ladder displaced from M13 DNA by heating. Without protein, there is minimal spontaneous displacement of DNA strands ~<40 bases from the substrate (lane 5), but E1HD is capable of dissociating DNA strands approaching 1000 bases, at the limits of the extension ladder (lanes 6–9). Again, we noted inhibition of unwinding at high-protein concentrations (lane 9). In the presence of the single-stranded binding protein RPA, unwinding by E1HD was more efficient and uninhibited at high-protein concentrations (lanes 11–14). We conclude from these experiments that recombinant E1HD is a 3′→5′

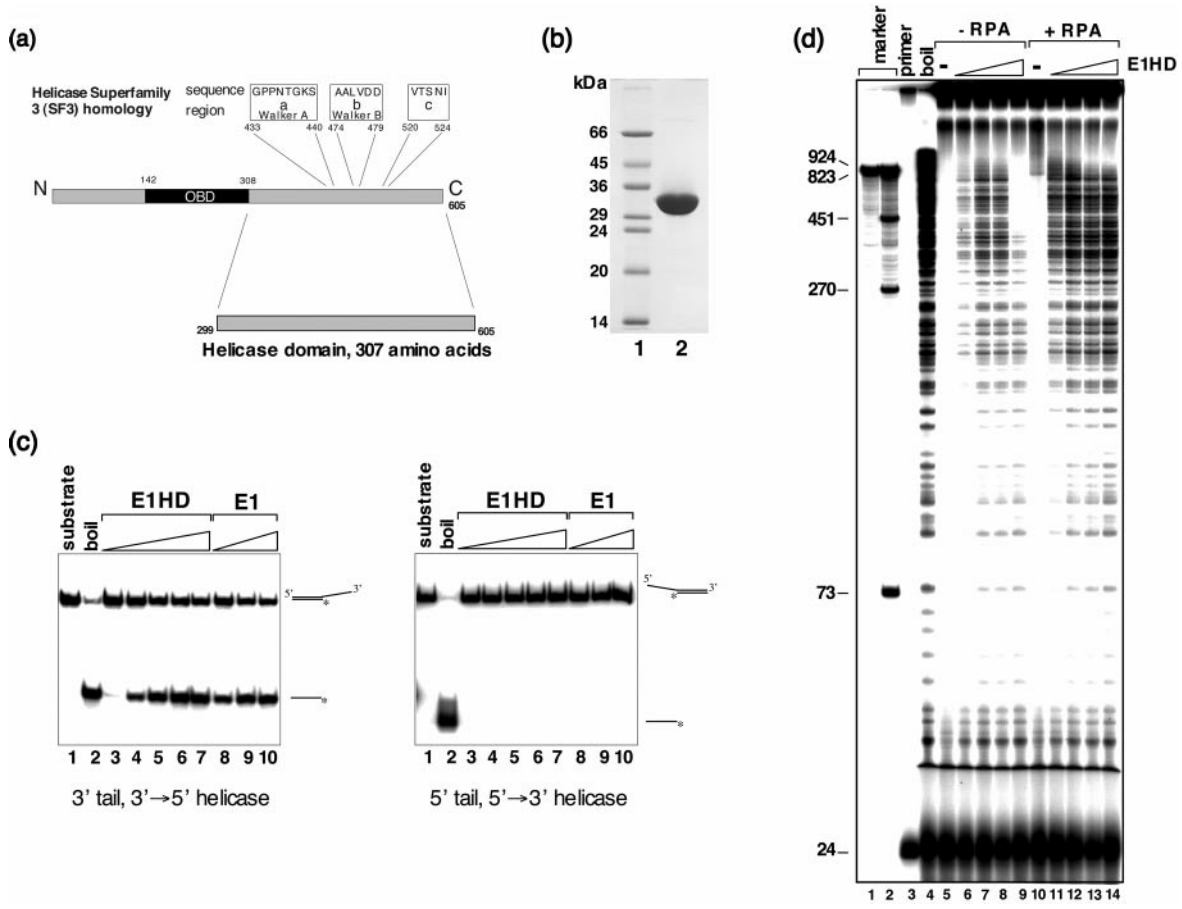

Figure 1. The BPV E1 helicase protein and DNA unwinding activity. (**a**) Schematic representation of BPV E1. The location of the sequence-specific origin DNA binding domain (OBD) and helicase domain (HD) are indicated. Conserved sequences of the helicase superfamily 3 and their location in E1 are indicated; all are critical for ATPase activity. The sequence alignment with SV40 and polyoma virus T-antigens begins at amino acid 327. (**b**) E1HD was expressed and purified to near homogeneity. Lane 2 shows 20 μg of protein on an SDS–polyacrylamide gel (12%, w/v). (**c**) Polarity of DNA unwinding. E1 and E1HD unwound substrates (64 bp dsDNA) with a base 3′ tail (left panel), but not a 5′ tail (right panel). Lanes 1 and 2: native and denatured substrates. Lanes 2–7: E1HD, 62.5, 125, 250, 500 and 1000 nM. Lanes 8–10: E1, 75, 150 and 300 nM. (**d**) Displacement of long DNA fragments generated by extension of a primer annealed to M13 DNA. Lanes 1 and 2: size marker generated from restriction fragments of known length. Lane 3: 24 base primer. Lane 4: boiled substrate. Lane 5: reaction with no protein. Lanes 6–9: 125, 250, 500 and 1000 nM E1HD. Lanes 10–14: as in lanes 5–9 except for the addition of RPA (56 ng/μl).

helicase capable of displacing long ssDNA strands from duplex DNA.

ssDNA-binding by E1HD

E1HD bound readily to ssDNA, with no apparent sequence preference (data not shown). The length-dependence of the E1HD interaction with ssDNA was investigated by gel-shift assays using ^{32}P-end-labelled poly-dT oligonucleotides of varying length (Figure 2). For the 30, 20, 18 and 16 base oligonucleotides (T30, T20, T18 and T16) we observed only a small difference in the extent of binding when incubated with an increasing concentration of protein (upper and middle panel). For the T14 and T12 oligonucleotides, binding was progressively impaired but detectable for the 12-base oligonucleotide (middle panel). Minimal complex formation with the poly(dT) oligonucleotides T10 and T8 was detectable upon prolonged exposure of the gel-shift gel, but no complex formed at all with oligonucleotide T6. The minimal binding site requirement for efficient ssDNA-binding by the E1HD is therefore ~16 bases. We also note that all complexes migrated similarly in the native gel system, suggesting that the same complex forms regardless of ssDNA size.

Figure 2b shows a comparison of E1HD binding to labelled T42, T30 and T18 oligonucleotides at high-protein concentrations. The small difference in binding affinity observed between the 18 compared with the 30 and 42 base oligonucleotides is evident as a complex instability in the gel, judged by the appearance of partially retarded probe in the image shown [compare lanes 2–4 (T18) with lanes 6–8 and 10–12 (T30 and T42)]. However, under solution reaction conditions the complex with the T18 oligonucleotide was found to be exceptionally stable (Figure 6).

E1HD forms a hexameric complex with ssDNA

To determine the oligomeric form of E1HD bound to ssDNA we performed gel filtration chromatography to give the Stokes' radius (Figure 3a) and glycerol gradient centrifugation the sedimentation coefficient of the protein–DNA complex (data not shown). When the E1HD protein alone was applied to a Superdex 200 gel filtration column at

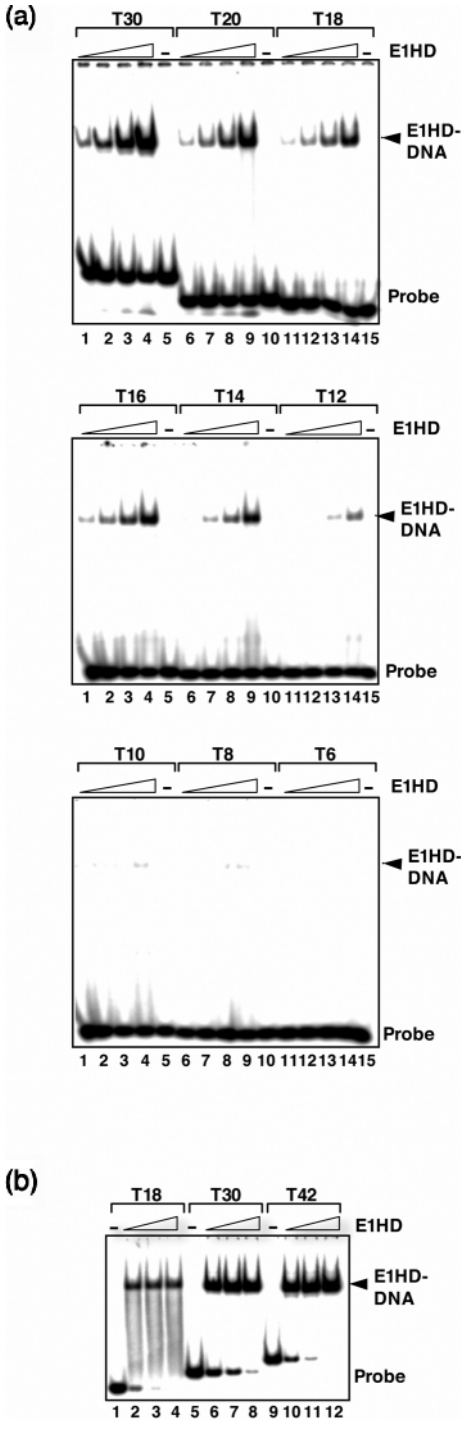

Figure 2. E1HD binding to synthetic poly(dT) oligonucleotides. (**a**) ssDNA size requirement for E1HD DNA binding. Poly(dT) oligonucleotides 6–30 bases in size were end-labelled for gel-shift analysis with E1HD, 0.25, 0.5, 1 and 2 μM. (**b**) Oligonucleotides ⩽18 bases form an unstable gel-shift complex. Binding of E1HD to T18, T30 and T42 probes is compared at high-protein concentration (2.5, 3.5 and 5 μM). Binding extents were similar except that the complex formed with the T18 oligonucleotide was unstable in the gel-shift gel, as evident from the broad band of partially retarded probe.

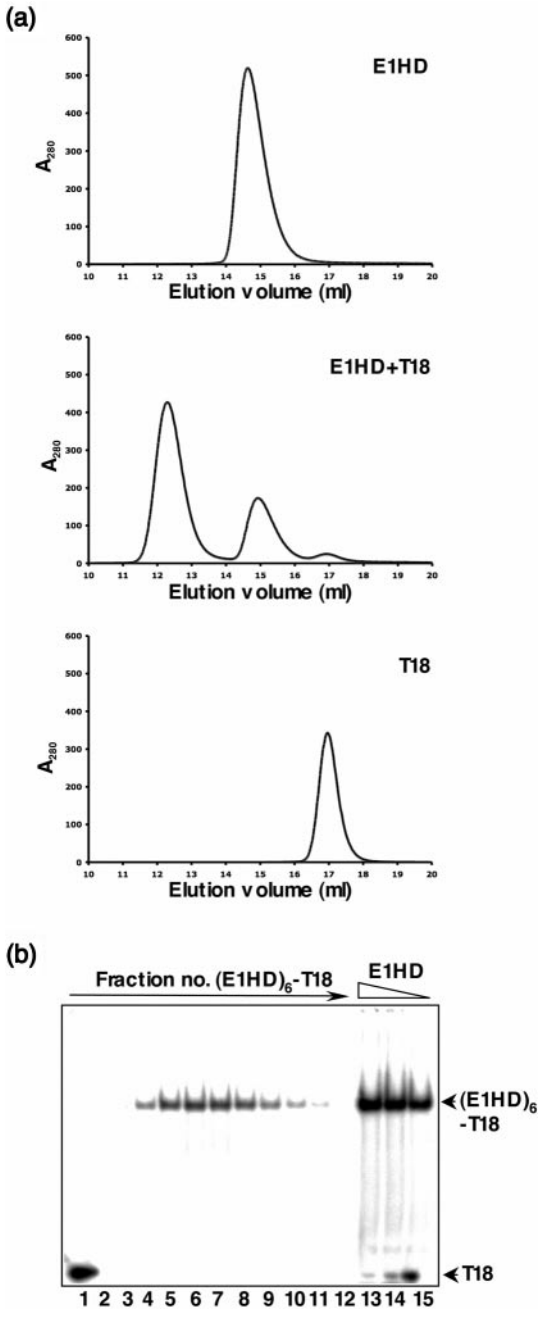

Figure 3. Molecular weight determination of the E1HD–DNA complex. (**a**) Representative gel filtration analysis (Superdex 200) of E1HD and a T18 oligonucleotide. Upper panel, absorbance at 280 nm for protein alone (6 mg/ml) plotted against elution volume. In the presence of T18 oligonucleotide an oligomeric complex formed (middle panel). The panel below shows the elution of T18 oligonucleotide from the column. (**b**) Analysis of gel filtration fractions of the oligomeric $(E1HD)_6$–T18 complex, formed with ^{32}P-labelled oligonucleotide, on a native polyacrylamide gel. Lane 1 is free probe. Lanes 2–12 are samples across the complex peak. Lanes 13–15 show the products of a *de novo*-binding reaction.

concentrations up to the 9 mg/ml tested, the protein eluted as a low molecular weight species (Figure 3a, upper panel, 6 mg/ml E1HD). The Stokes' radius of E1HD was found to be 33.3 ± 0.2 Å and the sedimentation coefficient 3.6 ± 0 S corresponding to a molecular mass of 45 ± 0.4 kDa, compared with 34.83 kDa predicted for a monomer. When E1HD was pre-incubated with the oligonucleotide T18 and applied to the gel filtration column, a high molecular weight complex formed (Figure 3a, middle panel), that did not form with oligonucleotide alone (lower panel). For this complex,

the Stokes' radius was found to be 56 ± 0.1 Å and the sedimentation coefficient 9.4 ± 0.4 S, corresponding to a molecular weight of 217 ± 14 kDa. To determine the stoichiometry of protein to DNA in the complex the protein and DNA content of the peak fraction were determined. These results gave a ratio of 5.9 ± 0.03 protein molecules per oligonucleotide. The predicted molecular weight of a hexameric E1HD complex bound to a T18 oligonucleotide is 214.8 kDa. These data are therefore consistent with a hexameric complex of E1 bound to a single molecule of T18 DNA, $(E1HD)_6$–T18.

We have previously reported that E1HD forms an oligomeric complex with ATP/Mg^{2+} in the absence of DNA (8). The elution volume of this complex by gel filtration (Superdex 200) was similar to the $(E1HD)_6$–T18 complex, indicating that it is also a hexamer. When E1HD was pre-incubated with ATP/Mg^{2+} over a range of concentrations and applied to the gel filtration column, hexamer formation was highly cooperative between 10 and 30 μM protein (0.35–1 mg/ml), but never reached 100% (data not shown). There was no indication of intermediate species, corresponding to dimers to pentamers, or species larger than hexamer, at any protein concentration tested. However, in glycerol gradients we failed to obtain a single discrete protein peak corresponding to hexamer, but observed protein from monomer through to hexamer (data not shown). With ADP/Mg^2 the protein was entirely monomeric at concentrations up to 10 mg/ml tested (data not shown). Similarly, the sedimentation profile of the protein in glycerol gradients containing AMP–PNP (adenylyl-imidodiphosphate) was indistinguishable from gradients containing no cofactor or ADP, indicating that the protein is also monomeric in the presence of the non-hydrolysable cofactor (data not shown).

The gel-shift assay provides a simple means of analysing binding, but information on protein–DNA stoichiometries are difficult to obtain. However, when the peak gel filtration fractions of $(E1HD)_6$–T18 formed with a ^{32}P-labelled oligonucleotide were analysed on a native gel, the complex co-migrated with the products of a independent *de novo* binding reaction (Figure 3b). In both the gel-shift analysis and hydrodynamic analysis of E1HD–ssDNA complexes there was little or no indication of multiple species. These results strongly suggest therefore that the complex we observe by gel-shift is also a hexameric E1HD complex.

Nucleotide cofactors and E1HD complex formation with ssDNA and dsDNA

The apparent binding affinity of E1HD for ssDNA (oligo T30 shown) is enhanced in the presence of ATP compared with its absence, as shown in Figure 4a, lanes 1–5 compared with 6–10. In the presence of the non-hydrolysable ATP analogue AMP–PNP, binding activity was reduced further compared with reactions with no cofactor (lanes 11–15 compared with 1–5). Binding extents in the presence of ADP (lanes 16–20) were similar to those observed without cofactor. All complexes migrated similarly in the native gel system, indicating that the same oligomeric complex forms under all conditions.

The binding pattern to a 30 bp T–A duplex was complex (Figure 4b). Without cofactor (lanes 1–5), with AMP–PNP (lanes 11–15) or with ADP (lanes 16–20), the amount of bound probe was reduced compared with reactions with T30 ssDNA. Multiple protein–DNA complexes formed, up to five distinct bands without cofactor, some of which were common to all binding reactions. With ATP two distinct complexes formed that were common to all reactions with and without cofactors. The pattern of binding with ATP however was mostly indicative of unstable protein–DNA complex formation, as evident from the appearance of a broad band of partially retarded probe (lanes 7–10).

The apparent equilibrium binding constants (K_d) for binding to the T30 oligonucleotide were determined with and without ATP, and sample data are shown in Figure 4c. Binding was cooperative and without cofactor a K_d of 1.83 ± 0.29 μM was determined, compared with 297 ± 7 nM in the presence of ATP.

ssDNA protection by the hexameric El complex

To characterize the E1HD–ssDNA interaction further we generated an internally ^{32}P-labelled 84 base probe and performed a gel-shift assay and nuclease protection assay in parallel. E1HD bound ssDNA in the presence or absence of ATP/Mg^{2+} as shown in Figure 5a. On this long probe, two shifted complexes were observed, and we note a mobility difference between complexes formed with and without ATP that was not observed on short probes. Products of the nuclease protection assay were analysed on denaturing sequencing gels as shown in Figure 5b. Lane 2 is the 84 base ssDNA probe. When E1HD was pre-incubated with ssDNA and ATP/Mg^{2+} and then treated with nuclease P1 and micrococcal nuclease for increasing time (lanes 3–5, 5, 15 and 30 min) the resulting cleavage products were not significantly different to reactions containing no E1HD (lanes 6–8). Only one weak product band of ~35 nt increased in intensity with digestion time (1*). However, for reactions performed without ATP/Mg^{2+}, lanes 9–14, the presence of E1HD resulted in a significant product of ~33 nt that was resistant to nuclease digestion (2*). Some products up to ~8 bases smaller also appeared (indicated with the bracket), as did a minor product of approximately twice the size (62–63 bases, 3*).

Cofactor modulation of the E1 hexamer ssDNA-binding site

The ability to observe discrete nuclease protection products, in the assay described above, only in the absence of ATP was surprising since ATP appears to promote complex formation. We investigated the stability of $(E1HD)_6$–ssDNA complexes by first pre-forming the complex with ^{32}P-labelled ssDNA without cofactor, then diluting the reaction in to buffer containing excess cold competitor and either ATP, ADP AMP–PNP or no cofactor. Reaction products were then cross-linked with glutaraldehyde before running on polyacrylamide gels. This measure was necessary since complex instability in the gel system was observed for short oligonucleotides (Figure 2b), and particularly apparent over long running times. Glutaraldehyde cross-linking did not alter the binding extents observed without cross-linking (data not shown). In Figure 6a the gel was run continuously over a period of 4 h. Lane 1 is free probe, lane 2 is a control reaction where competitor and radiolabelled T18 DNA were mixed before adding protein, and lane 3 shows the products of the initial binding reaction. Without cofactor (lanes 4–7), with

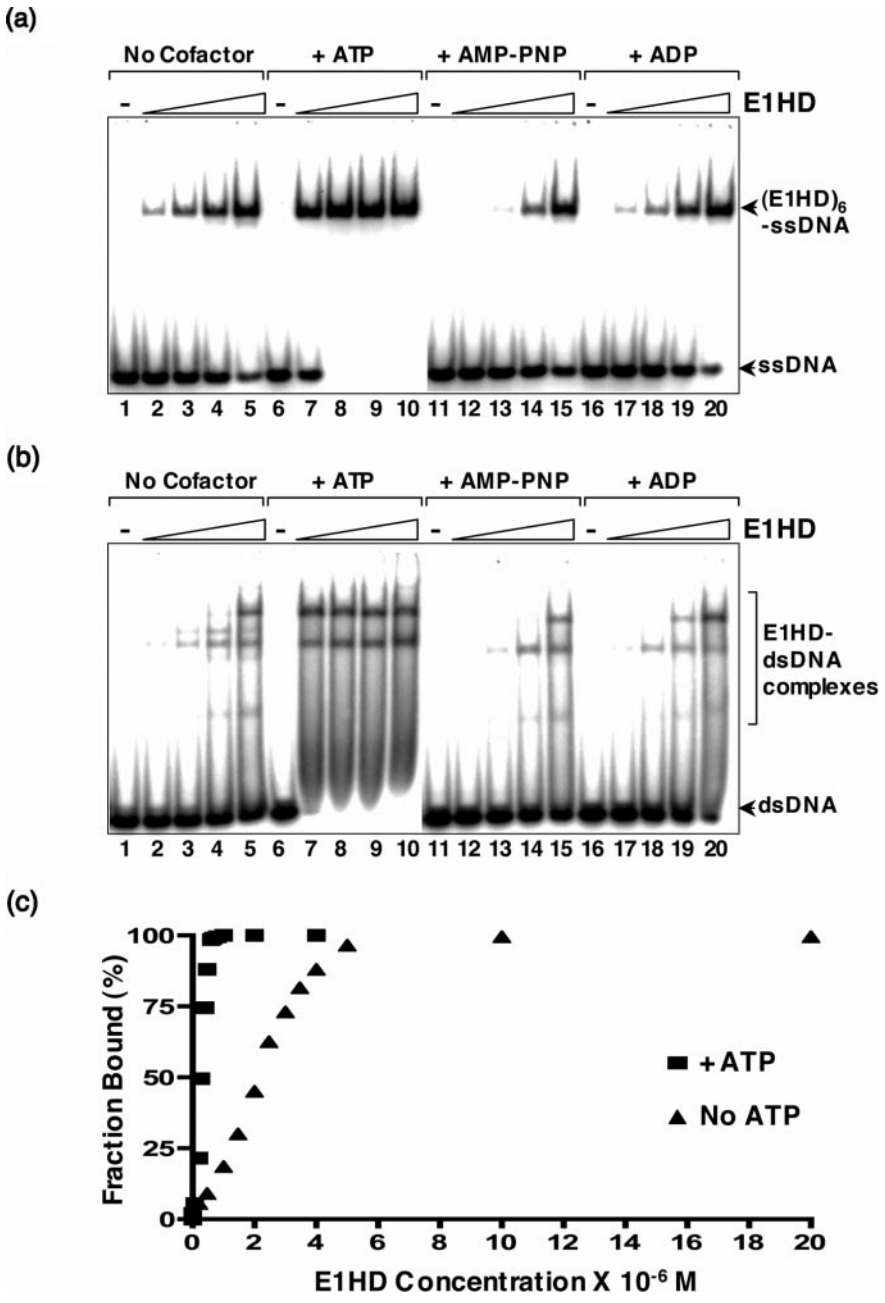

Figure 4. Cofactor dependent binding of E1HD to ss- and dsDNA. (**a**) Binding to oligonucleotide T30. E1HD was titrated from 0.25, 0.5, 1 and 2 μM. Lanes 1–5, no cofactor; lanes 6–10, complex formation with ATP; lanes 11–15, complex formation with AMP–PNP; and lanes 16–20, addition of ADP. (**b**) Binding to a 30 base poly(dT)–poly(dA) duplex. Reactions were assembled as in (a) above. (**c**) Determination of equilibrium binding constants (K_d) for the $(E1HD)_6$–T30 interaction. Sample data are shown for reactions with ATP (0.05–4 μM E1HD) and without (0.25–20 μM E1HD).

ADP (lanes 8–11), or AMP–PNP the $(E1HD)_6$–T18 complex was exceptionally stable. For all reactions we were unable to determine any appreciable decay of the complex over the 4 h time course shown, and even up to 6 h also (data not shown). However, in the presence of ATP we observed remarkably different kinetics, as shown in Figure 6b, where the time course was >6 min. Within the first 30 s after the addition of ATP 70–75% of the T18 complex dissociates, then the rate of complex dissociation steadily declines (Figure 6b and c). With the T30 and T42 oligonucleotide similar results were obtained except that ~50% of the complex dissociated in 60 s (Figure 6c). The dissociation kinetics did not fit simple single- or biphasic decay models.

Oligomerization assembles a catalytically robust protein complex

We next asked if the protein concentration dependence of oligomerization in the presence of ATP observed by gel filtration and described above was reflected in the ATPase activity of E1HD. Initial rates of ATP hydrolysis were measured over a range of protein concentrations and ATP

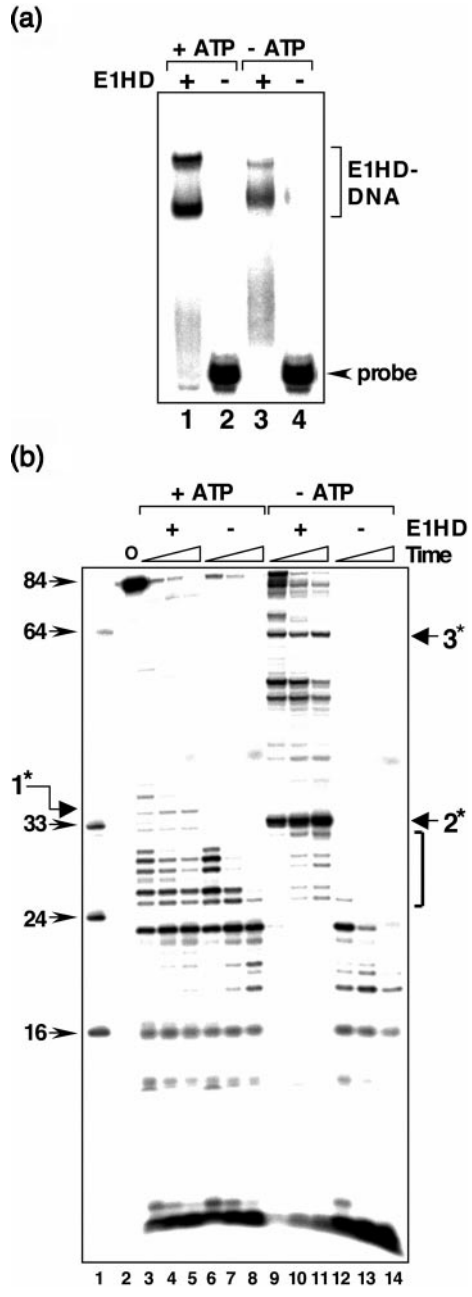

Figure 5. ssDNA protection by E1HD with and without ATP. (**a**) Reactions were assembled with an internally ^{32}P-labelled 84 base ssDNA probe (5 nM) with (lanes 1 and 2) and without ATP (lanes 3 and 4) and analysed by gel-shift. Two complexes were observed with the long probe that were not observed with shorter probes. (**b**) Reactions were treated with a mixture of micrococcal and P1 nucleases and digestion products analysed on denaturing sequencing gels after 5, 15 and 30 min. Lane 1, marker lane generated with oligonucleotides of known length. Lane 2, probe alone. Lanes 3–5 and 6–8, reactions with ATP, with and without E1HD, respectively. A faint product band of ~35 bases (1*) appeared in reactions with E1HD. Without ATP (lanes 9–14) two discrete protection products of 33 (2*) and ~60 (3*) bases were observed in the presence of E1HD. Minor species of lower molecular weight were found in association with the major product (indicated with the brackets).

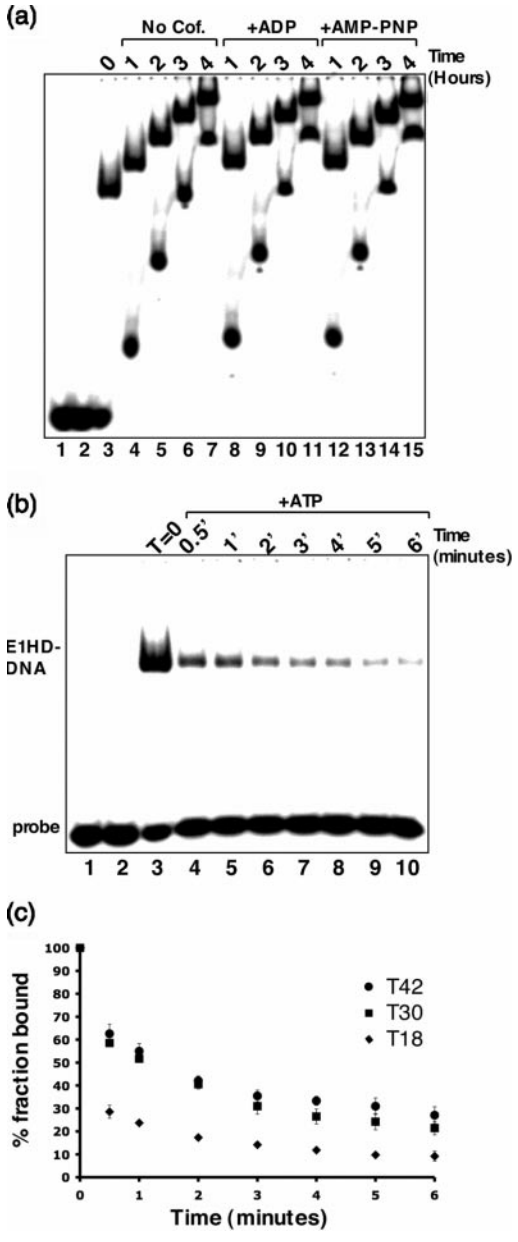

Figure 6. Stability of $(E1HD)_6$–ssDNA complexes with or without nucleotide cofactors. DNA-binding reactions were assembled without cofactor (3.5 μM E1HD, 4 nM probe T18 shown in this case), pre-incubated (15 min) and diluted 2-fold into reactions containing no cofactor, ADP, AMP–PNP or ATP (5 mM each), and 200 μM T20 competitor DNA (~350-fold excess over E1HD hexamer). Reactions were sampled at time intervals and cross-linked with glutaraldehyde for gel-shift analysis. (**a**) Reactions without cofactor (lanes 4–7), with ADP (lanes 8–11), and AMP–PNP (lanes 12–15). Lane 1 shows free probe, lane 2 control reaction with competitor (200 μM T20) added before addition of the protein, and lane 3 is the products of the binding reaction before division, dilution and addition of competitor and cofactors. Reactions were sampled at 1, 2, 3 and 4 h, cross-linked and applied to a continuously running gel. (**b**) Reactions with ATP. Lanes 1–3, as in (a) above. Lanes 4–10, reactions sampled at 0.5, 1, 2, 3, 4, 5 and 6 min. (**c**) Data from three independent experiments are plotted for the T18 oligonucleotide shown above, but also a 30mer (T30) and 42mer (T42).

hydrolysed per nmol of protein per second plotted against protein concentration as shown in Figure 7a (dashed line). There was a sigmoidal dependence of ATPase activity on protein concentration, where the ATP hydrolysed per protein molecule increases up to ~50 μM E1HD. At 50 μM protein, 0.264–0.294 mol of ATP are hydrolysed per mol of protein per second (k_{cat} = 0.28/s). In the presence of ssDNA, ATP hydrolysis was stimulated at low protein concentrations

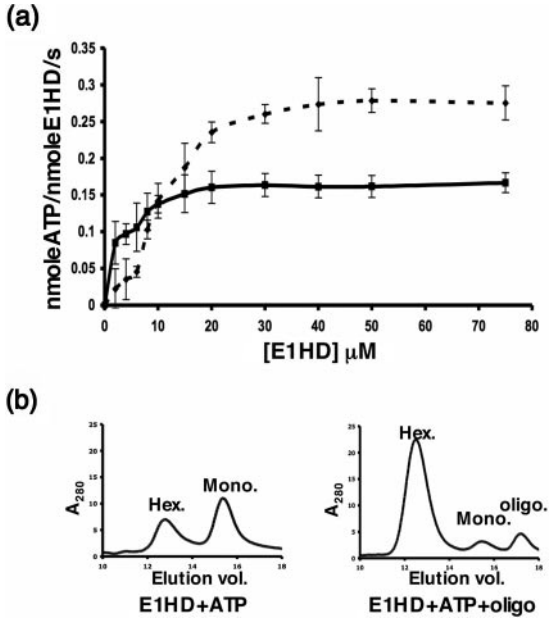

Figure 7. Hexamerization assembles a catalytically robust ATPase complex. (**a**) ATPase activity as a function of E1HD protein concentration. Reactions were assembled with (solid line) and without oligonucleotide (dashed line) and P_i released determined after 3 min at 22°C. (**b**) Oligonucleotide stimulates E1HD hexamerization in the presence of ATP. At 17.4 μM ~40% of the E1HD protein is in the oligomeric form (left) and oligonucleotide stimulates oligomerization (right).

(solid line), and no further increase in the catalytic constant was observed ~>30 μM protein. However, the catalytic constant was lower than that observed in the absence of ssDNA (0.16 s^{-1}). We addressed the mechanism of ssDNA stimulation of ATPase activity by analysing hexamerization of E1HD at low protein concentrations in the presence of oligonucleotide (Figure 7b). At 17.4 μM E1HD ~40% of the protein incubated in the presence of ATP and applied to a gel filtration column is oligomeric. However, in the presence of ssDNA, formation of the oligomeric complex was stimulated. In similar reactions without ATP, none of the protein was in the hexameric form at this protein concentration, with or without oligonucleotide (data not shown). The results of the gel filtration analysis are thus in accord with the gel-shift analysis in Figure 4. Together, these results indicate that ATP is required to assemble a hexameric E1HD complex with high catalytic activity.

DISCUSSION

The C-terminal 307 residue domain of BPV E1 (E1HD) functions as a helicase with the unwinding polarity of native E1. E1HD was capable of displacing long DNA strands from duplex DNA (Figure 1d), and based on our studies we propose below a mechanism for transclocase activity and processive unwinding by a hexameric protein complex. The enzyme is monomeric at high-protein concentrations without cofactor or with ADP. In the presence of ATP oligomerization is highly cooperative. Consistent with the properties of other members of the same helicase family the complex appears to be hexameric, as its elution volume in gel filtration was similar to the hexameric complex with ssDNA whose size we determined accurately. The nucleotide requirements for oligomerization therefore resemble those for full-length E1 binding to double-stranded *ori* DNA, where the complexes that form in the absence of hydrolysable ATP are relatively unstable (29). It is curious however that hexamerization of full-length E1 itself has not been observed with ATP (22,23). It is possible that the protein concentrations required for hexamerization were not achieved in previous studies or that the experimental conditions did not favour complex stabilization. Hydrolysis of available ATP is a likely explanation for our inability to observe discrete peaks in glycerol gradients (data not shown), performed over hours rather than minutes in the case of gel filtration. We have also shown that oligomerization in the presence of ATP is required to assemble a catalytically robust ATPase. Many AAA+ helicases proteins possess an 'arginine finger' (31,32), first identified in GTPases (33). In some multimeric ATPase complexes the finger from one subunit extends into another to interact with the ATP tri-phosphate during hydrolysis. T-antigen has an unusual finger motif in that a lysine as well as two arginines contact the phosphate directly or indirectly through a water molecule (34). A conserved arginine in HPV 18 E1 is required for robust ATPase activity and is possibly an arginine finger residue (35). The cooperative ATPase activity we observe therefore supports the notion that the papillomavirus helicase is an arginine finger ATPase. Furthermore, since E1–E2 interactions are conserved between BPV and HPV, the ATP-driven oligomerization of BPV E1HD we describe could serve as a molecular mechanism for the displacement of E2 from E1 during initiator complex assembly, as in HPV (35). It is also noteworthy that SV40 T-antigen hexamerizes with ATP, ADP and non-hydrolysable ATP analogues (21), and that HPV 11 E1 apparently forms stable hexamers without cofactors or DNA (24). Despite the sequence conservation and predicted structural similarity between T-antigen and E1, subtle differences may exist in the ATP hydrolysis cycle of these two viral helicases. Within the papillomaviruses E1 proteins there may also be differences in the enzyme mechanism.

E1HD binds ssDNA as a hexamer with only one molecule of an 18 base oligonucleotide (T18) per complex. Thirty-three bases of ssDNA were protected from nuclease digestion by the helicase and only small differences in the binding affinity of poly(dT) oligonucleotides from 16 to 30 bases were observed. Formation of the hexameric complex was significantly impaired for oligonucleotides of ⩽14 bp. The 16 base DNA sequence therefore defines the extent of the ssDNA required for hexamerization, whereas the length of protected DNA indicates passage of DNA through a protein complex larger than the minimal ssDNA-binding site. Very stable hexameric complexes formed with an 18 base oligonucleotide (T18) but these were unstable under electrophoresis conditions compared with hexamers with a T30 oligonucleotide (Figure 2b). Together with the results of the protection assay, this suggests that stabilizing contacts with nucleic acid may also occur outside an essential DNA-binding site. These results are similar to those of other well-studied hexameric helicases such, as T7 gp4, that protect 25–30 bases of ssDNA (36). T7 gp4 and DnaB bind short oligonucleotides (10–30 bases) in the presence of non-hydrolysable ATP

analogues with K_ds of 10 and 60 nM, respectively (36–38). Both these helicases also bind a second DNA strand with a weaker K_d, ~40 μM in the case of DnaB. The binding constants (K_d) that we have obtained for E1, with or without ATP, are significantly higher, between those of the primary and secondary binding sites of DnaB. However, the mechanism of helicase loading on DNA is different for these enzymes. E1 and T-antigen bind and assemble on DNA via the sequence-specific OBD, while specific proteins load DnaB and T7 gp4 on to ssDNA. The E1HD binding to dsDNA that we observe is complex, with no clear indication of the efficient and stable hexamerization seen with ssDNA. Although T-antigen and E1 encircle their respective *ori* dsDNAs as hexamers, this is performed in conjunction with the OBD. T7 gp4, DnaB and T-antigen both exclude one ssDNA strand during helicase unwinding (15,18,20), and E1 is likely to function similarly. Together with the inability of E1HD to unwind DNA of pure duplex character, our dsDNA-binding data suggest that E1 is unlikely to translocate on dsDNA as a base pair separation machine.

E1HD forms an exceptionally stable complex with ssDNA oligonucleotides without cofactor, with ADP or with AMP–PNP. However, upon ATP addition the affinity for ssDNA is significantly reduced. The ATP-dependent kinetics of $(E1HD)_6$–ssDNA complex dissociation we observed (Figure 6) showed an immediate phase of rapid dissociation followed by a slower rate of decay. These observations are notable since ATP stimulates formation of the hexameric protein–DNA complex. With NTP compared with NDP or no cofactor T7 gp4 and DnaB also bind ssDNA more tightly, by orders of magnitude (36,38), and in the case of DnaB, nucleotide is not required for hexamerization (39). The immediate questions that arise are how is ssDNA affinity modulated and can these results be rationalized in terms of current models for DNA unwinding? ssDNA complex dissociation could occur if the hexameric ring were to open or disassemble. We consider these possibilities unlikely since we show that ATP promotes protein complex assembly. Furthermore, the mechanism of E1 helicase loading occurs by stepwise binding to *ori* rather than loading of a preformed hexamer requiring a ring-opening step. Our favoured interpretation is that we have observed the ATP-dependent modulation of ssDNA-binding site affinity that is a component of the helicase transloction mechanism. The recent structures of T-antigen hexamers with and without bound nucleotide have shown large longitudinal ATP-dependent movements of a β-hairpin structure (the pre-sensor 1 β hairpin, PS1βH) within the central channel of the complex (34). This structure is critical for ssDNA binding in both T-antigen and E1 hexamers (7,8), and along with an aromatic loop constitutes the primary ssDNA-binding site. PS1βH movement is accompanied by changes in the dimensions of the hexameric channel, rotation of the two tiers of the hexamer relative to each other, and a large increase in the buried surface area between protomers with ATP (34). These data also suggested that the ATP hydrolysis cycle was all-or-none, with all protomers transducing the energy of ATP hydrolysis in a concerted step. The initial rapid dissociation of ssDNA, we observed, upon ATP addition may represent PS1βH movement, ssDNA translocation, and its consequential release from the binding site at the end of the hydrolysis cycle. Changes in the DNA-binding site from high to low affinity must occur or the helicase would not move. The subsequent decrease in the ssDNA complex dissociation rate is not consistent with the rapid turnover of ATP by E1HD that we measured, albeit that ATPase activity is reduced in the prersence of ssDNA (Figure 7). However, this may be the result of accumulating ADP, or a slow rate of ADP release from the helicase–ssDNA complex, suggesting that translocase activity itself cannot be effectively reconstituted on ssDNA alone. With T-antigen, the excluded ssDNA and a small region of dsDNA ahead of a replication fork also interact with the helicase, and all ATP modulated interactions may require coupling for efficient use of ATP and unwinding/translocation. With T-antigen, the excluded ssDNA has been shown to load on the outside of the helicase at high ATP concentrations (19). Our observation that a small mobility difference in gel-shifts is seen for E1HD complexes loaded onto large ssDNA probes with or without ATP (Figure 5a), may indicate that ssDNA can also interact with the exterior of the E1 hexamer in a cofactor dependent manner.

In summary, our data suggest that during the ATP-hydrolysis cycle an internal ssDNA-binding site in an E1 hexamer oscillates from a high to a low-affinity state while protein–protein interactions change from a low- to high-affinity state. This mechanism would ensure that the complex remains tethered to DNA while processive movement along DNA proceeds. A complete evaluation of this proposal awaits the determination of the crystal structures of E1 or T-antigen with DNA. These data would also provide an answer to the intriguing question of how the path of DNA through the complex impacts on the assembly of stable hexameric structures.

ACKNOWLEDGEMENTS

We thank Jon Sayers and James Chong for critical reading of the manuscript. This work was supported by a grant from Yorkshire Cancer Research to C.M.S. Funding to pay the Open Access publication charges for this article was provided by Yorkshire Cancer Research.

Conflict of interest statement. None declared.

REFERENCES

1. Dean,F.B., Bullock,P., Murakami,Y., Wobbe,C.R., Weissbach,L. and Hurwitz,J. (1987) Simian virus 40 (SV40) DNA replication: SV40 large T antigen unwinds DNA containing the SV40 origin of replication. *Proc. Natl Acad. Sci. USA*, **84**, 16–20.
2. Wold,M.S., Li,J.J. and Kelley,T.J. (1987) Initiation of simian virus 40 DNA replication *in vitro*: large-tumour antigen- and origin-dependent unwinding of the template. *Proc. Natl Acad. Sci. USA*, **84**, 3643–3647.
3. Yang,L., Mohr,I., Fouts,E., Lim,D.A., Nohaile,M. and Botchan,B. (1993) The E1 protein of bovine papillomavirus 1 is an ATP-dependent DNA helicase. *Proc. Natl Acad. Sci. USA*, **90**, 5086–5090.
4. Seo,Y.-S., Muller,F., Lusky,M. and Hurwitz,J. (1993) Bovine papillomavirus (BPV)-encoded E1 protein contains multiple activities for BPV DNA replication. *Proc. Natl Acad. Sci. USA*, **90**, 702–706.
5. Borowiec,J.A. and Hurwitz,J. (1988) Localised melting and structural changes in the SV40 origin of replication induced by T-antigen. *EMBO J.*, **7**, 3149–3158.
6. Gillette,T.G., Lusky,M. and Borowiec,J.A. (1994) Induction of structural changes in the bovine papillomavirus type 1 origin of replication by the viral E1 and E2 proteins. *Proc. Natl Acad. Sci. USA*, **91**, 8846–8850.

7. Shen,J., Gai,D., Patrick,A., Greenleaf,W.B. and Chen,X. (2005) The roles of the residues on the channel β-hairpin and loop structures of simian virus 40 hexameric helicase. *Proc. Natl Acad. Sci. USA*, **102**, 11248–11253.
8. Castella,S., Bingham,G. and Sanders,C. (2006) Common determinants in DNA melting and helicase catalysed DNA unwinding by papillomavirus replication protein E1. *Nucleic Acids Res.*, **34**, 3008–3019.
9. Stenlund,A. (2003) Initiation of DNA replication: lessons from viral initiator proteins. *Nat. Rev. Mol. Cell. Biol.*, **4**, 777–785.
10. Sedman,J. and Stenlund,A. (1995) Co-operative interaction between the initiator E1 and the transcriptional activator E2 is required for replicator specific DNA replication of bovine papillomavirus *in vivo* and *in vitro*. *EMBO J.*, **14**, 6218–6228.
11. Schuck,S. and Stenlund,A. (2005) Assembly of a double hexameric helicase. *Mol. Cell*, **20**, 377–389.
12. Sanders,C.M. and Stenlund,A. (2000) Transcription factor dependent-loading of the E1 initiator reveals modular assembly of the papillomavirus origin melting complex. *J. Biol. Chem.*, **275**, 3522–3524.
13. Mastrangelo,I.A., Hough,P.V., Wall,J.S., Dodson,M., Dean,F.B. and Hurwitz,J. (1989) ATP-dependent assembly of double hexamers of SV40 T-antigen at the viral origin of DNA replication. *Nature*, **338**, 658–662.
14. Egelman,E.H., Yu,X., Wild,R., Hingorani,M.M. and Patel,S.S. (1995) Bacteriophage T7 helicase/primase forms rings around single-stranded DNA that suggests a general structure for hexameric helicases. *Proc. Natl Acad. Sci. USA*, **92**, 3869–3873.
15. Hacker,K.J. and Johnson,K.A. (1997) A hexameric helicase encircles one DNA strand and excludes the other during DNA unwinding. *Biochemistry*, **36**, 14080–14087.
16. Bujalowski,M. and Jezewska,M.J. (1995) Interactions of *Escherichia coli* primary replicative helicase DnaB protein with single-stranded DNA. The nucleic acid does not wrap around the protein hexamer. *Biochemistry*, **34**, 8513–8519.
17. Ayora,S., Weise,F., Mesa,P., Stasiak,A. and Alonso,J.C. (2002) *Bacillus subtilis* bacteriophage SPP1 hexameric DNA helicase, G40P, interacts with forked DNA. *Nucleic Acids Res.*, **30**, 2280–2289.
18. SenGupta,D.J. and Borowiec,J.A. (1992) Strand-specific recognition of a synthetic DNA replication fork by the SV40 large tumour antigen. *Science*, **256**, 1656–1661.
19. Smelkova,N.V. and Borowiec,J.A. (1998) Synthetic DNA replication bubbles bound and unwound with twofold symmetry by a simian virus 40 T-antigen double hexamer. *J. Virol.*, **72**, 8676–8681.
20. Jezewska,M.J., Rajendran,S. and Bujalowski,W. (1997) Strand specificity in the interaction of *Eschericia coli* primary replicative helicase DnaB protein with a replication fork. *Biochemistry*, **36**, 10320–10326.
21. San Martin,M.C., Gruss,C. and Carazo,J.M. (1997) Six molecules of SV40 T antigen assemble in a propeller-shaped partical around a channel. *J. Mol. Biol.*, **268**, 15–20.
22. Sedman,J. and Stenlund,A. (1998) The papillomavirus E1 protein forms a DNA-dependent hexameric complex with ATPase and DNA helicase activities. *J. Virol.*, **72**, 6893–6897.
23. Fouts,E.T., Yu,X., Egelman,E.H. and Botchan,M.R. (1999) Biochemical and electron microscopic image analysis of the hexameric E1 helicase. *J. Biol. Chem.*, **274**, 4447–4458.
24. White,P.W., Pelletier,A., Brault,K., Titolo,S., Welchner,E., Thauvette,L., Fazekas,M., Cordingley,M.G. and Archambault,J. (2001) Characterization of recombinant HPV6 and 11 E1 helicases: effect of ATP on the interaction of E1 with E2 and mapping of a minimal helicase domain. *J. Biol. Chem.*, **276**, 22426–22438.
25. Patel,S.S. and Picha,K.M. (2000) Structure and function of hexameric helicases. *Annu. Rev. Biochem.*, **69**, 651–697.
26. Sedman,T., Sedman,J. and Stenlund,A. (1997) Binding of the E1 and E2 proteins to the origin of replication of bovine papillomavirus. *J. Virol.*, **71**, 2887–2896.
27. Iggo,R.D. and Lane,D.P. (1989) Nuclear protein p68 is an RNA-dependent ATPase. *EMBO J.*, **8**, 1827–1831.
28. Henricksen,L.A., Umbricht,C.B. and Wold,M.S. (1994) Recombinant replication protein A: expression, complex formation, and functional characterisation. *J. Biol. Chem.*, **269**, 11121–11132.
29. Sanders,C. and Stenlund,A. (1998) Recruitment and loading of the E1 initiator protein: an ATP-dependent process catalysed by a transcription factor. *EMBO J.*, **17**, 7044–7055.
30. Li,M. and Desiderio,S. (1993) Physical characterisation of DNA binding proteins in crude preparations. In Harris,E.L.V. and Angal,S. (eds), *Transcription Factors: A Practical Approach*. IRL Press, Oxford University Press, Oxford, UK, pp. 185–196.
31. Sawaya,M.R., Guo,S., Tabor,S., Richardson,C.C. and Ellenberger,T. (1999) Crystal structure of the helicase domain from the replicative helicase-primase of bacteriophage T7. *Cell*, **99**, 167–177.
32. Singleton,M.R., Sawaya,M.R., Ellenberger,T. and Wigley,D.B. (2000) Crystal structure of T7 gene 4 ring helicase indicates a mechanism for sequential hydrolysis of nucleotides. *Cell*, **101**, 589–600.
33. Ahmadian,M.R., Stege,P., Scheffzek,K. and Wittinghofer,A. (1997) Confirmation of the arginine-finger hypothesis for the GAP-stimulated GTP-hydrolysis reaction of Ras. *Nat. Struct. Biol.*, **4**, 686–689.
34. Gai,D., Zhao,R., Li,D., Finkielstein,C.V. and Chen,X. (2004) Mechanism of conformational change for a replicative hexameric helicase of SV40 large tumour antigen. *Cell*, **119**, 47–60.
35. Abbate,E.A., Berger,J.M. and Botchan,M.R. (2004) The X-ray structure of the papillomavirus helicase in complex with its molecular matchmaker E2. *Genes Dev.*, **18**, 1981–1996.
36. Hingorani,M.M. and Patel,S.S. (1993) Interactions of bacteriophage T7 DNA primase/helicase protein with single-stranded and double-stranded DNAs. *Biochemistry*, **32**, 12478–12487.
37. Jezewska,M.J., Rajendran,S. and Bujalowski,W. (1998) Functional and structural heterogeneity of the DNA binding site of the *Escherichia coli* primary replicative helicase DnaB protein. *J. Biol. Chem.*, **273**, 9058–9069.
38. Jezewska,M.J. and Bujalowski,W. (1996) Global conformational transitions in *Escherichia coli* primary replicative helicase DnaB protein induced by ATP, ADP, and single-stranded DNA binding. Multiple conformational states of the helicase hexamer. *J. Biol. Chem.*, **271**, 4261–4265.
39. Bujalowski,W., Klonowska,M.M. and Jezewska,M.J. (1994) Oligomeric structure of *Escherichia coli* primary replicative helicase DnaB protein. *J. Biol. Chem.*, **269**, 31350–31358.